Scripta Materialia 154 (2018) 30–33

Contents lists available at ScienceDirect

Scripta Materialia

journal homepage: www.elsevier.com/locate/scriptamat

Regular article

An ultrahigh strength and enhanced ductility cold-rolled medium-Mn steel treated by intercritical annealing

Xuan Li, Renbo Song *, Naipeng Zhou, Jiajia Li

School of Materials Science and Engineering, University of Science and Technology Beijing, Beijing 100083, China

A R T I C L E I N F O

Article history:
Received 18 April 2018
Received in revised form 10 May 2018
Accepted 11 May 2018
Available online xxxx

Keywords:
Medium manganese steel
Intercritical annealing
Austenite
Ferrite
Mechanical properties

A B S T R A C T

An ultrahigh strength and enhanced ductility cold-rolled medium-Mn steel was manufactured via intercritical annealing. The fine lamellar and equiaxed duplex microstructure, austenite (40.5 vol%) and ferrite, was observed due to austenite reversed transformation and ferrite recrystallization. The ultimate tensile strength (1090.0 MPa), total elongation (56.3%) and product of strength and elongation (PSE) (61.4 GPa·%) were achieved, which were comparable and superior to the reported medium-Mn steels. The excellent properties were attributed to high dislocation density, transformation induced plasticity, twinning induced plasticity, grain refinement strengthening and solution strengthening effects. Additionally, the dependence of PSE on austenite fraction was discussed.

Medium-Mn steels, with 5%–12% Mn containing, have been proposed as the third generation advanced high strength steels (AHSS) in automotive application due to their ultrahigh strength with little compromise of ductility [1]. Recently, intercritical annealing (IA) has been generally adopted as a heat treatment practice to generate the ultrafine-grained structure in medium-Mn steel. By conducting the heat treatment above, researches [2–6] reported that the mechanical properties of medium-Mn steels including ultimate tensile strength (UTS), yield strength (YS), total elongation (TE) and the product of UTS × TE (PSE) greatly varied in wide ranges of 906–1420 MPa, 530–714 MPa, 20–63% and 20–60 GPa·%, respectively. Such a variation is mainly attributed to different austenite fractions and stabilities, which are critical targets to determine whether or what strong strain hardening mechanism will happen in austenite grains during deformation. Sohn et al. [7] developed a novel ferrite-austenite duplex medium-Mn steel with UTS of 734 MPa and great TE of 77% due to the occurrence of both transformation induced plasticity (TRIP) effect and twinning induced plasticity (TWIP) effect during deformation. It has been reported that fine dislocation structures formed by high-dislocation-density walls as well as planar glide configuration significantly promote the strength [8]. Furthermore, the addition of alloy elements obviously enhanced the strength through several conventional methods, such as solution strengthening and precipitation strengthening. Cai et al. [9] investigated Fe-6.5Mn-1.1Al-0.17C steel with 0.22 wt% Mo and 0.05 wt% Nb addition, achieving UTS of 1224 MPa and TE of 33%. He et al. [10] discovered that the addition of 0.7 wt% V contributes to the forming of intensive nanoscale V-carbides, providing enhanced resistance to delay fracture induced by hydrogen embrittlement. However, the alloy elements addition subsequently brings about some problem in cost and difficulty in manufacturing. In this work, a cold-rolled medium-Mn steel with low row-materials cost was designed and heat treated by IA. A high PSE (61.4 GPa·%) was achieved with ultrahigh strength and enhanced ductility, which is superior to reported medium-Mn steels. The relationship between properties and microstructure was discussed by microstructure characterization and mechanical performance testing. Besides, the function of austenite and dislocations during deformation were emphasized, and meanwhile, special interest was focused on the strengthening and ductility-enhancing mechanisms of present steel.

The chemical composition of present steel is Fe-7.75Mn-2.78Al-0.52C (wt%). A 20 kg cast of this steel is produced using an induction melting furnace and forged into a billet ingot with a diameter of 35 mm. The ingot is homogenized at 1180 °C for 2 h, followed by hot rolling into 4-mm-thick strips with UTS of 1375.8 MPa and TE of 5.9%. Before cold rolling (CR), annealed at 700 °C for 60 min is necessary for dislocation recovery and ferrite recrystallize to ensure over 60% CR-reduction. Hence, 1.5-mm-thick CR sheets are manufactured with ultrahigh UTS of 2005.7 MPa and TE of 6.6%. Then, the CR sheets are IA at 700 °C for 30 min following by air cooling to room temperature. Tensile tests are carried out at room temperature with the strain rate of 10^{-3} s^{-1} and the specimens are cut along rolling direction with the gauge of 25 mm and a width of 6 mm. The microstructure is analyzed by transmission electron microscopy (TEM) and electron back-scatter diffraction (EBSD). Energy dispersive spectrometer (EDS) is used to investigate the element distribution and X-ray diffraction (XRD) is used to measure

* Corresponding author.
E-mail address: songrb@mater.ustb.edu.cn (R. Song).

https://doi.org/10.1016/j.scriptamat.2018.05.016

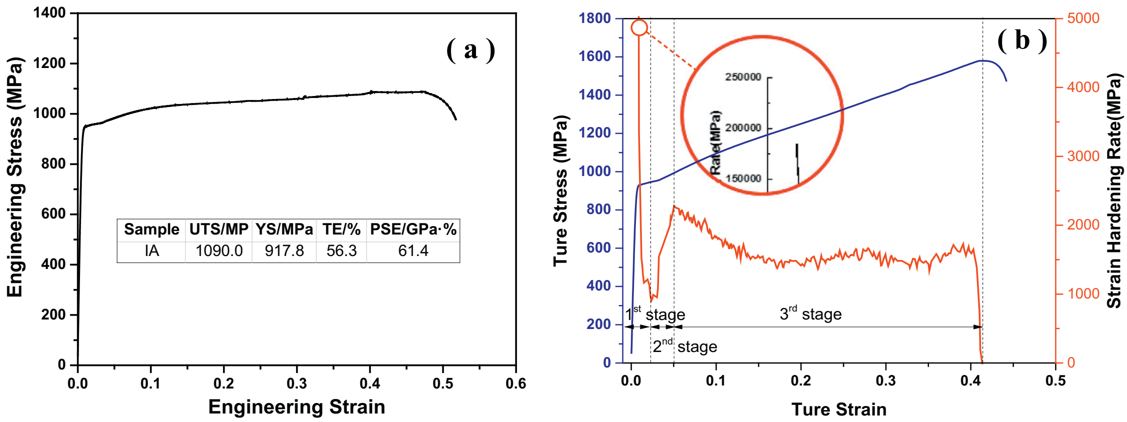

Fig. 1. The engineering stress-strain curve (a), true stress-strain curve and corresponding stain-hardening rate curve (b) of IA specimen.

the fraction of retained austenite. The calculations for determining the volume fraction of austenite are based on the integrated intensities of $(200)_{bcc}$, $(211)_{bcc}$, $(200)_{fcc}$, $(220)_{fcc}$ and $(311)_{fcc}$ diffraction peaks.

Fig. 1a shows the engineering stress-strain curve of the specimen subjected to IA, which exhibits continuous yielding without yielding point or Lüders bands. The IA specimen has excellent mechanical properties, with UTS of 1090.0 MPa, YS of 917.8 MPa, TE of 56.3% and PSE of 61.4 GPa·%. Fig. 1b shows the true stress-strain curve, together with stain-hardening rate (SHR) curve. The IA specimen shows a three-stage strain hardening behavior, i.e. the SHR firstly decreases (stage I), then increases slightly (stage II) at 3% true strain before decreasing again (stage III) at 5% true strain. It has been reported [2,11] that stage I is associated with deformation of ferrite, stage II is governed by TRIP effect and stage III is the results of the co-work among ferrite, austenite and newly formed martensite. It is worth noting that the SHR at initial deformation shows a super high level of about 190 GPa, indicating the outstanding strain hardening capacity of present steel.

Austenite and ferrite duplex microstructure were obtained in IA specimen before tensile test, both of which exhibit two types of morphology: lamellar and equiaxed (Fig. 2a). 40.5 vol% of austenite was obtained with average grain size of 0.64 μm (Fig. 2b). Some large austenite grains were decorated with dislocation lines and inclined grain boundaries (Fig. 2c). Randomly distributed tangled dislocations were observed in equiaxed ferrite (Fig. 2c). The thicknesses of lamellar ferrite is 190.0 nm, where the dislocation cells were found (Fig. 2d). The thicknesses of lamellar austenite is 437.3 nm, where the dislocations were found as well (Fig. 2d). It is noted that the dislocation density in lamellar grains is much higher than that in equiaxed ones. Besides, Mn contents

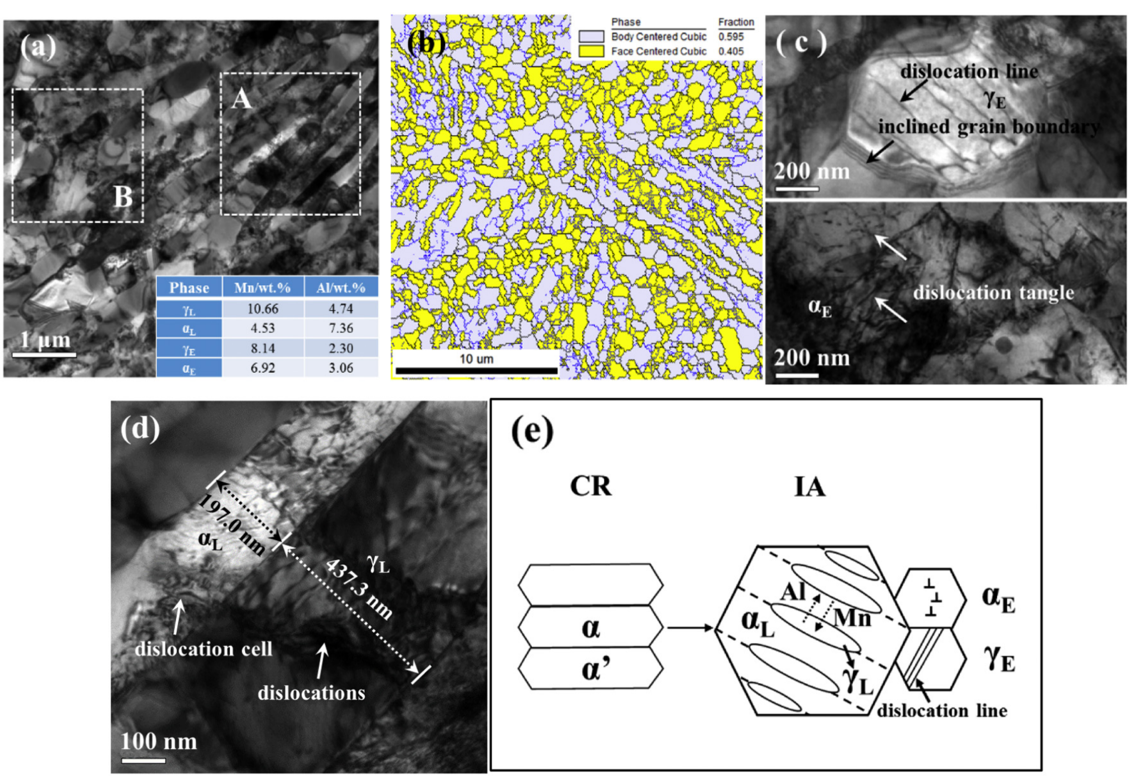

Fig. 2. Microstructure of IA specimen before tensile test. (a) TEM observation showing both the austenite and ferrite grains exhibit two types of morphology marked by dotted rectangle: zone A lamellar; zone B equiaxed; (b) EBSD phase image, austenite was revealed by yellow and ferrite was presented by gray; (c) Dislocations in equiaxed microstructure; (d) The amplification of lamellar microstructure; (e) Sketches of the microstructure evolution during IA. "γ_E" and "α_E" represent the equiaxed austenite and ferrite grains; "γ_L" and "α_L" represent the lamellar austenite and ferrite grains; "α" and 'α" represent the ferrite and martensite. (For interpretation of the references to colour in this figure legend, the reader is referred to the web version of this article.)